Research on Chemical Intermediates (2025) 51:839–873
https://doi.org/10.1007/s11164-024-05473-5

Exploring Schiff base ligand and their transition metal complexes: synthesis, characterization, antimicrobial, ADME and computational insight as cholesterol lowering agents and anticancer activity on HeLa cells

Indu Sindhu[1] · Anshul Singh[1] · Yogesh Deswal[2] · Jagat Singh Kirar[3]

Received: 8 August 2024 / Accepted: 30 November 2024 / Published online: 21 December 2024

Abstract

This research work includes a detailed investigation of the synthesis, spectroscopic characterization and biological properties of Schiff bases ligand derived from 1,8-diamminonapthalene and 5-bromosalicyaldehyde along with their transition metal complexes. The compounds were meticulously characterized employing sophisticated spectral techniques that are FT-IR (Infra-red), analytical, ^{1}H-NMR (Proton Nuclear Magnetic Resonance), SEM (Surface morphology analysis), ESI–MS (Electrospray Ionization Mass Spectrometry), PXRD (Powder X-ray Diffraction) and ESR (Electron Spin Resonance). The spectroscopic data reported that the ligand exhibits a tetradentate binding mode, while the metal complexes demonstrate hexa-coordinated geometries. Additionally, DFT investigation was executed employed B3LYP/LanL2DZ as basis set to optimize geometry and evaluate molecular electrostatic potential surfaces. In vitro antimicrobial studies were explored against gram +ve bacteria, gram −ve bacteria and fungal strains. Among these, the copper chloride complex (3) displayed the highest efficacy possessing a minimum inhibitory concentration (MIC) of 0.0094 µmol/mL. Molecular docking investigations were executed to evaluate the binding affinities of the synthesized compounds against a cholesterol lowering agent (2OBD) and HeLa cancerous cells (6I2I). The results indicated that cobalt (1) and nickel chloride (2) complexes exhibit the lowest binding affinities, suggesting higher potency. Additionally, the synthesized compounds demonstrated greater effectiveness against HeLa cancerous cells compared to the 2OBD receptor. The in silico ADME analysis discloses the therapeutic usability of the synthesized compounds.

Extended author information available on the last page of the article

Graphical abstract

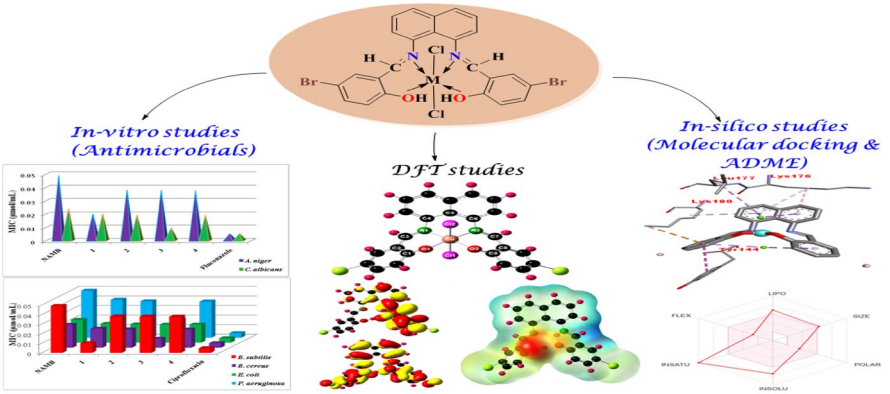

Keywords Anticancer agents · Molecular docking · Antimicrobial activity · ADME studies · DFT studies · Schiff base transition metal complexes

Introduction

Flexible ligands, frequently referred to as Schiff bases, possess the potential to synthesize complexes with transition metal ions that proven beneficial in a variety of domains, such as photophysical research, biology, optics, magnetic chemistry, chemical analysis and catalysis [1–10]. A growing body of scientific evidence reveals that transition metal ions are crucial for carry out vital biological functions [11]. The justification for this is that many drugs action depend on either suppressing the growth of metalloenzymes or coordinating with metal ions [12]. Coordination compounds combine the ability of metals to interact with various kinds of organic ligands or mixed ligands with a broad spectrum of coordination numbers, geometries and oxidation states [13, 14]. The emergence of drug-resistant microbial infections is the main contributing factor to the current restrictions on the administration of antibiotics in the treatment of microbial ailments [15–17]. Schiff base complexes have grown progressively more significant in medicine as potential alternatives in contrast to the standard antibiotics [18–21].

In order to create anticancer medications that are efficient, pharmaceutical industries have conducted extensive studies throughout the years [22–28]. Over the course of the last twenty years, there has been a lot of engrossment in the discipline of chemistry of metal complexes [29–35]. Numerous transition metal complexes have already been developed and investigated for their potential for tackling cancer [36–39]. In the same class as carboplatin and cisplatin, oxaliplatin is a platinum-based anticarcinogenic medication. However, it has some restrictions because major side effects include diarrhea, tiredness, sickness, apathy and a low blood cell count. Several attempts have consequently been made to employ several different ligands

or transition metals in place of this medication with the objective of swapping it for worthy substitutes [40–42]. Diverse pharmacological properties have been demonstrated by these complexes, such as antimicrobic, anti-inflammatory, anticancer, herbicidal, antioxidant and chemo/biosensing [43–53]. Due to their propensity to obstruct many enzymatic activities and to induce noteworthy tumor preference, Schiff base ligands have garnered a lot of fascination in the treatment of cancer over the preceding few decades [54–57]. Such ligands heteroatom-incorporated compounds offer a stronger propensity for bimolecular interaction [58]. Such chemicals have demonstrated their biological relevance in inhibiting bacterial growth against strains of *E. coli* that induce marine biofilms [59].

One of the prominent underlying components of hypercholesterolemia that causes cardiovascular disorders is the absorption of cholesterol from the diet. The endogenous production of cholesterol among human beings is attributed to the mevalonate pathway. The reaction HMG-CoA to mevalonate catalyses by enzyme 3-hydroxy-3-methylglutaryl-coenzyme A reductase (HMGR), that assists in the generation of cholesterol. The identification of therapeutic targets is a crucial step in the procedure of drug screening and development. One of the key targets for the regulation of cholesterol production is HMGR [60]. The ultimate objective of this scientific investigation is to discover new agents that will effectively lower down free cholesterol levels by inhibiting HMGR, address drug resistance and lessen the challenges posed by current medication side effects.

In an effort to generate Schiff base metal complexes having anticancer properties along with cholesterol lowering characteristics, we have prepared Schiff base ligand along with its transition metal complexes and characterized their structure via several spectral techniques. To get insight into their antimicrobial relevance, in vitro antimicrobial assay was assessed against the selected bacterial and fungal strains. To explore their anticancer proficiency on HeLa cancerous cells and cholesterol lowering characteristics, molecular docking was demonstrated which unveils their biological effectualness against both receptor proteins. However, druglikeness was evaluated by ADME studies revealing their drug-like properties.

Experimental details

Apparatus techniques

An FT-IR spectrophotometer with KBr pellets as support was used to acquire infrared spectra in the 400–4000 cm^{-1} range. At SAIF-IIT Bombay, an electromagnetic spin resonance (ESR) investigation was carried out using equipment from Varian (USA). At GJUST-Hisar, the electrospray ionization spectrum was recorded for all synthesized metal complexes. Powder X-ray diffraction investigations were carried out in the 10°–80° scanning range using a Rigaku Minifex-II instrument. At SAIF, Punjab University, Chandigarh, elemental analysis (CHN) was conducted through the EuroEA elemental analyzer. The surface morphology of metal complexes was examined using a FE-SEM instrument with a 15-kV accelerating voltage.

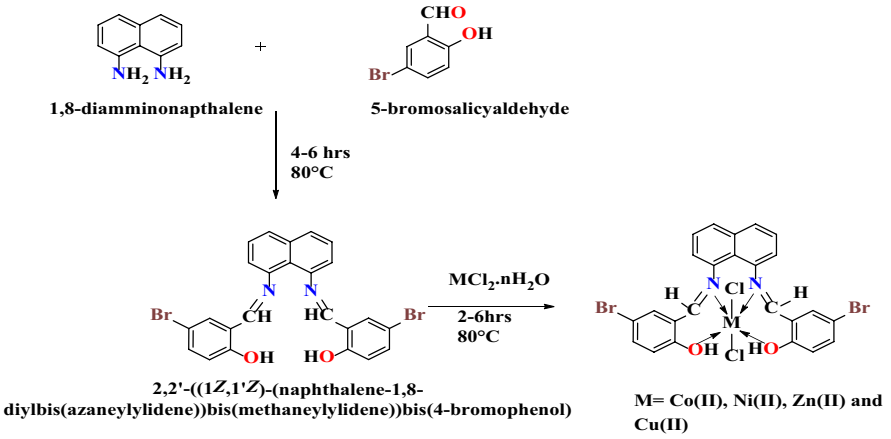

Scheme 1 Reaction methodology for the fabrication of Schiff base ligand and their metal complexes

General reagents

We procured the chloride salts of $ZnCl_2$(dry), $CuCl_2{\cdot}2H_2O$, $NiCl_2{\cdot}6H_2O$ and $CoCl_2{\cdot}6H_2O$ from MolyChem, India. The compounds utilized were 3-hydroxy-4-methoxybenzaldehyde and 1,8-diamminonapthalene which were retrieved from Sigma-Aldrich. Reagent-grade solvents were utilized, and no additional purification was performed.

Synthetic methodology

Synthetic methodology of the ligand

The condensation approach was implemented to fabricate the ligand [61]. The ethanolic solution of 1,8-diamminonapthalene was first dissolved in 5 mmol of ethanol prior to the addition of 10 mmol of 5-bromosalicyaldehyde and then heated to 70–80 °C. The reaction mixture was constantly refluxed at 80 °C for approximately 4–5 h. A solid precipitate with yellow color was attained. After filtering the resultant precipitate, the reactants that remained unreacted were removed by washing thoroughly with the ethanol.

Synthetic methodology of the metal complexes

To the heated solution of 0.25 mmol $ZnCl_2/CuCl_2{\cdot}2H_2O/NiCl_2{\cdot}6H_2O/CoCl_2{\cdot}6H_2O$ in 10 mL of absolute ethanol, slowly add 0.25 mmol of Schiff base ethanolic solution in a 1:1 ratio. The initiation of complex formation was shown by a color shift that occurred when the reactants were mixed. At 80 °C, the reaction mixture was constantly refluxed while being magnetically agitated for 2–6 h. To get rid of contaminants, the resulting colored precipitate was filtered and purified**.**

The reaction methodology is represented in Scheme 1.

Molecular docking studies

All the synthesized compounds and ligand were docked against cholesteryl ester transfer protein (2OBD) that is cholesterol lowering agent [62] and refined 13pf HeLa cell tubulin microtubule (6I2I), a receptor of HeLa cells responsible for the cervical cancer in womens [63–66]. Protein structures were gathered from the RCSB-protein data bank, and Open Babel software was used to transform the complex structures into pdb format. Autodock Tools was the software employed for the ligand root detection and grid box construction. The binding energy at RMSD 0.00 was determined after the docking was completed in AutoDockVina [67]. Pymol and Biovia Discovery Studio Visualizer were used to generate the three-dimensional structure.

Antimicrobial studies

The antimicrobial in vitro examination was accomplished against various microbes such as gram +ve bacteria (*B. subtilis*, *B. cereus*), gram −ve bacteria (*E. coli*, *P. aeruginosa*) as well as fungal strains (*A. niger*, *C. albicans*), and their minimum inhibitory concentration was evaluated [68, 69]. The ligand and synthesized compounds have been investigated for microbial efficacy adopting the liquid broth method of serial dilutions. Common drugs utilized during investigations for antifungal and antibacterial agents, respectively, are fluconazole and ciprofloxacin. Prepare a stock solution with concentration of 100 g/mL, 1 mg of sample was dissolved in 10 mL of dimethyl sulfoxide. Next, we gradually lowered the solution's concentration to 3.125 g/mL. Consequently, 1 mL of nutrient-rich broth and potato dextrose broth (PDB) were combined with the stock solution. While fungal strains were grown in PDB tubes for two days at 25 °C, identical bacterial strains were put in NB tubes and incubated at 37 °C for one day.

DFT studies

The density functional theory (DFT) assessment of the ligand and metal complexes were evaluated utilizing the Gaussian 09W program [70] with B3LYP functional [71–73], while the LanL2DZ basis set was employed for C, H, O and Co metal ion [74–76]. The estimation was performed implementing the similar method and basis set based on geometries optimization of ground state and other structure parameters such as bond lengths and bond angles. The molecular geometry of ligand and complexes has been fully optimized, and several quantum chemical descriptors and MEPs were all considered.

ADME studies

The online SWISSADME program was utilized to discover the drug-like characteristics of the synthesized complexes. This software estimates biological activity

based on the structure–activity relationship and displays activity versus over 3000 pharmacological effects and biochemical characteristics. The probable activity (P_a) and probable inactive activity (P_i) associated with this activity are expressed. Compounds that have been declared effective against that specific pharmacological action are those with a P_a value greater than P_i. Compounds with a P_a value of more than 0.5 have been proposed to be competent to demonstrate biological effects in vitro.

Results and discussion

The novel Schiff base ligand 2,2′-((naphthalene-1,8-diylbis(azaneylylidene)) bis (methaneylylidene)) bis (4-bromophenol) has been fabricated by reflux condensation reaction, and their transition metal complexes was prepared by further condensation reaction of Schiff base ligand with the metal chloride salts. The analytical data of the compounds were displayed in Table 1.

Infra-red spectra

The ligand infrared spectrum displays a broad band near 3350 cm^{-1} attributes to the phenolic OH group, while band around 3043 cm^{-1} was designated to the imine –CH aromatic group. The arrival of azomethine peak at 1606 cm^{-1} confirms the formation of ligand (Fig. 1). The other peaks owing to –C=C–, –C–O, –C–Br was observed at 1473 cm^{-1}, 1370 cm^{-1} and 813 cm^{-1} wavenumber. In the cobalt chloride metal complex (1), peak appeared in 1588 cm^{-1} wavenumber attributed to the azomethine linkage and the peak in 2960 cm^{-1} appeared due to azomethine –C–H bond. The deprotonation of OH group is found missing as revealed by the presence of OH peak in the metal complexes that appeared in 3390 cm^{-1}in the cobalt complex. The peaks of –C=C–, –C–O, –C–Br was discovered at 1467 cm^{-1}, 1365 cm^{-1} and 825 cm^{-1}. In nickel metal complex (2), peaks owing to CH=N, –C–H, –OH, –C=C–, –C–O– and –C–Br bonding divulges at wavenumber 1593 cm^{-1}, 3050 cm^{-1}, 3390 cm^{-1}, 1482 cm^{-1}, 1360 cm^{-1} and 815 cm^{-1}, respectively. The

Table 1 Analytical data of the synthesized ligand and metal complexes

Comp	Mol. formula	Mol. wt.	Yield (%)	Color	Cal. (Found)			
					C (%)	H (%)	N (%)	M (%)
NAMB	$[C_{24}H_{16}Br_2N_2O_2]$	524.21	78	Brown	54.99 (54.59)	3.08 (2.90)	5.34 (5.10)	–
(1)	$[C_{24}H_{16}Br_2N_2O_2CoCl_2]$	654.05	68	Crème	44.07 (43.98)	2.47 (2.34)	4.28 (4.10)	9.01 (8.91)
(2)	$[C_{24}H_{16}Br_2N_2O_2NiCl_2]$	653.81	60	Green	44.09 (43.80)	2.47 (2.34)	4.28 (4.12)	8.98 (8.70)
(3)	$[C_{24}H_{16}Br_2N_2O_2CuCl_2]$	658.66	72	Black	43.77 (43.66)	2.45 (2.30)	4.25 (4.20)	9.65 (9.52)
(4)	$[C_{24}H_{16}Br_2N_2O_2ZnCl_2]$	660.49	58	Crème	43.64 (43.46)	2.44 (2.20)	4.24 (4.10)	9.90 (9.76)

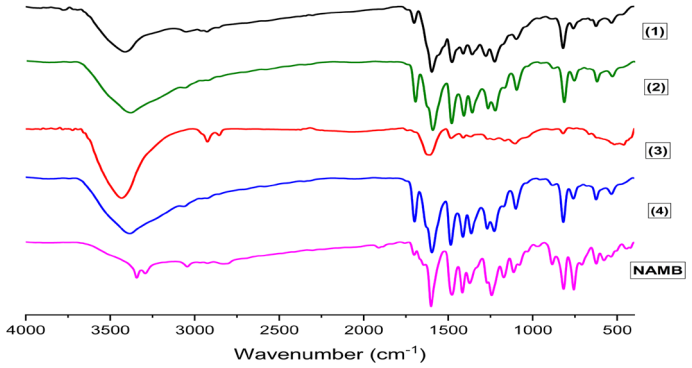

Fig. 1 IR spectra of the synthesized ligand and metal complexes

copper metal complex (3) exhibits peaks described for the –CH=N, –C–H, –OH, –C=C–, –C–O– and –C–Br bonds at 1516 cm^{-1}, 3042 cm^{-1}, 3416 cm^{-1}, 1470 cm^{-1}, 1365 cm^{-1} and 814 cm^{-1} correspondingly. The zinc chloride complex (4) evidences the peaks at 1590 cm^{-1}, 3052 cm^{-1}, 3378 cm^{-1}, 1480 cm^{-1}, 1360 cm^{-1} and 815 cm^{-1} attributes to –CH=N, –C–H, –OH, –C=C–, –C–O– and –C–Br bonding [77–86].

ESI–MS spectra

The mass spectrum of the Schiff base ligand (NAMB) exhibits a base peak at 524.95 amu which corresponds to $[M]^+$, while in cobalt chloride complex (1) peaks appear at 653.25 amu corresponding to $[M+H]^+$ ions peak. In case of nitrate chloride complex peaks discovered at 650.46 amu corresponds to $[M\text{-}3H]^+$. The zinc chloride molecular peak perceived at 658.48 amu attributes to $[M\text{-}2H]^+$ ion peak. The copper chloride displays $[M\text{-}5H]^+$ peak at 653.25 amu (Fig. 2).

^{1}H-NMR spectra

The ^{1}H-NMR spectra of Schiff base ligand displays peaks at δ 10.22 and 10.9 ppm which correlates with the –OH group of phenol while peak at δ 8.24 ppm attributes to the azomethine linkage, δ 6.52–7.73 ppm describes to the aromatic protons and peak of solvent protons ascribed at δ 3.35 ppm. The ^{1}H-NMR spectrum of the zinc chloride complex (4) exhibits peaks at δ 10.79 ppm, δ 8.21 ppm and δ 6.69–7.80 ppm which is ascribed to the phenolic –OH group, azomethine linkage and aromatic protons, respectively (Fig. 3).

ESR spectrum

The ESR spectrum was executed to analyze the magnetic characteristics of the copper chloride complex (Fig. 4). The copper complex exhibits isotropic signal at room

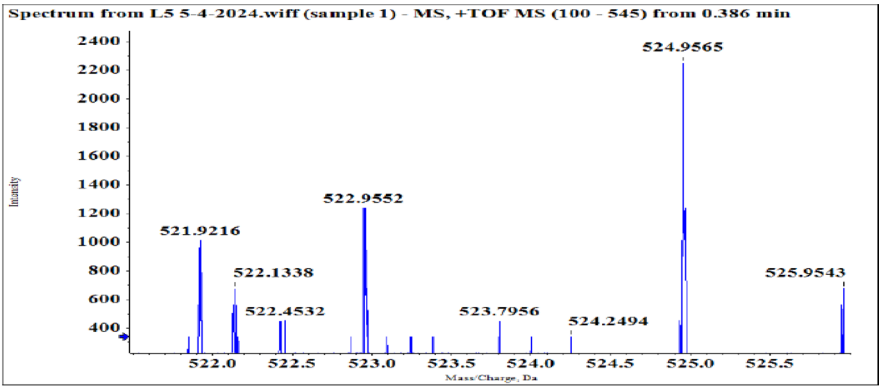

a) NAMB

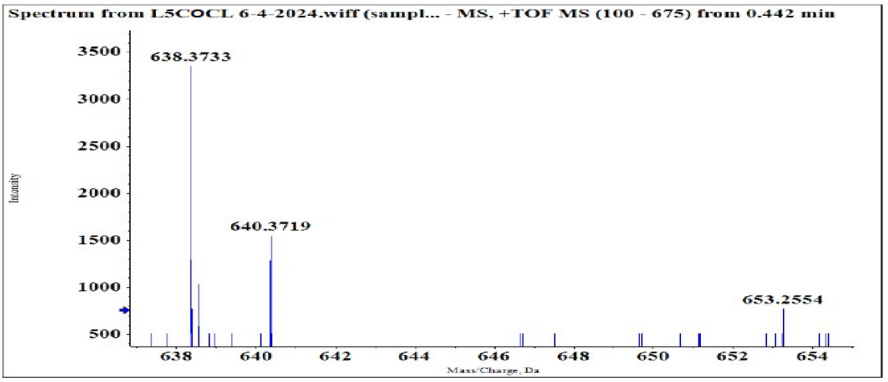

a) (1)

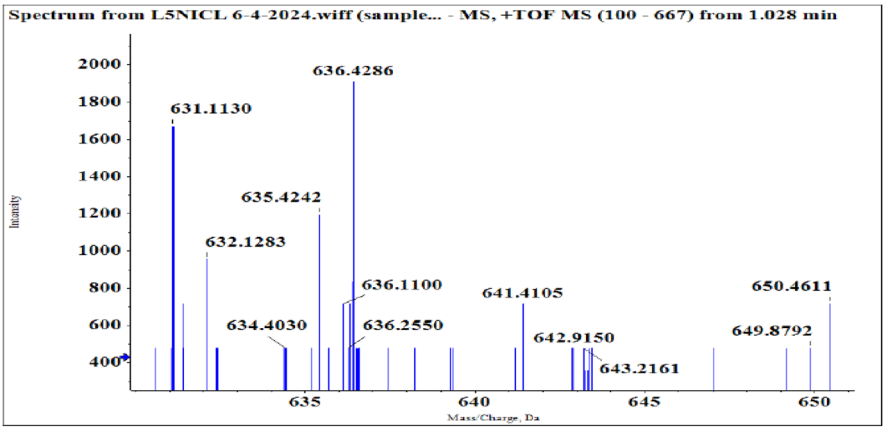

b) (2)

Fig. 2 Mass spectrum of the synthesized ligand and metal complexes

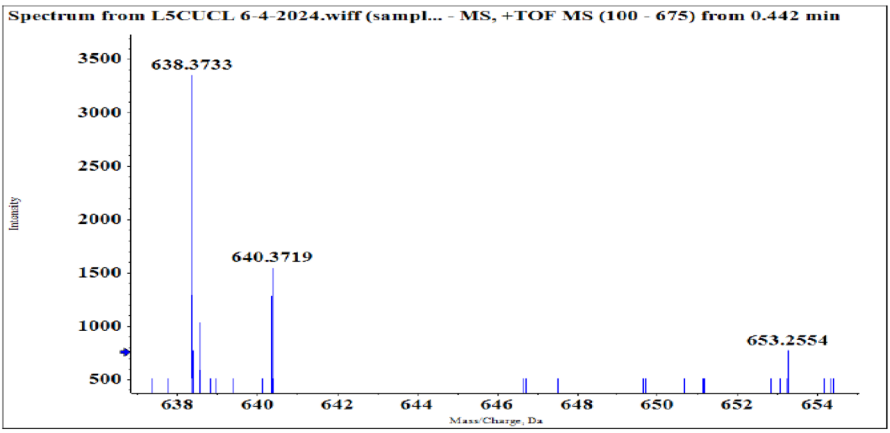

c) (3)

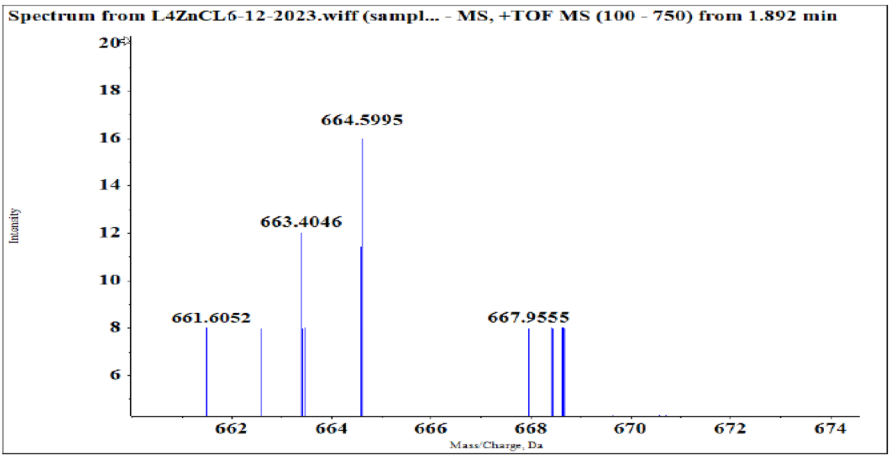

d) (4)

Fig. 2 (continued)

temperature with zero hyperfine splitting. The value of g_{iso} observed for copper chloride was 2.04. This value proclaimed that the unpaired electron resides in $d_{x^2-y^2}$ orbital with distorted octahedral geometry. The μ_{eff} was evaluated for the synthesized copper chloride complex, and the value obtained was 1.76 B.M. which confirms the paramagnetic nature of copper complex [87–89].

PXRD studies

The copper chloride complex was studied in 10°–80° range of 2θ angle having a wavelength of 15.4 nm because no single crystal was obtained for the synthesized compounds. The powder X-ray diffraction uncovered the fact that there are no peaks

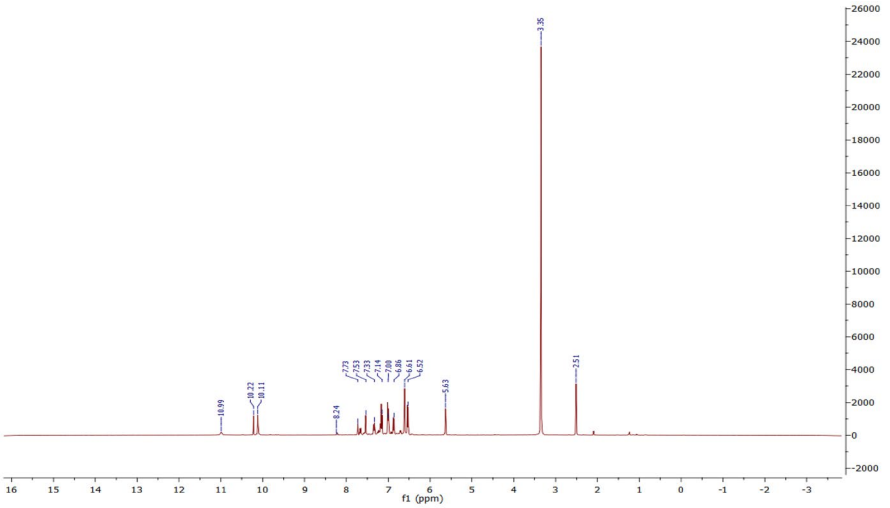

a) NAMB

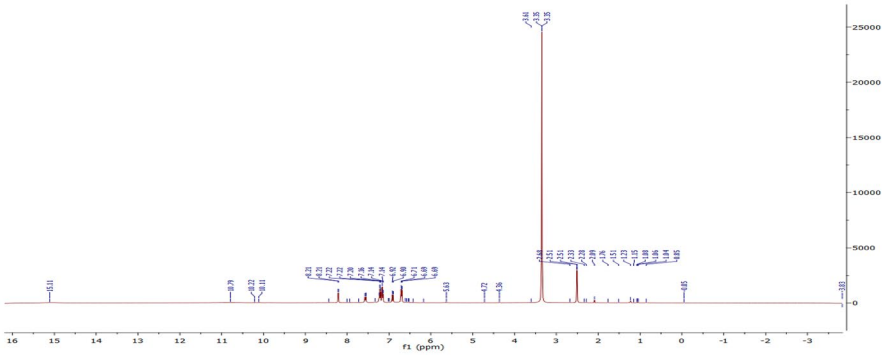

b) Zinc chloride

Fig. 3 [1]H-NMR spectra of **a** ligand and **b** zinc chloride complex

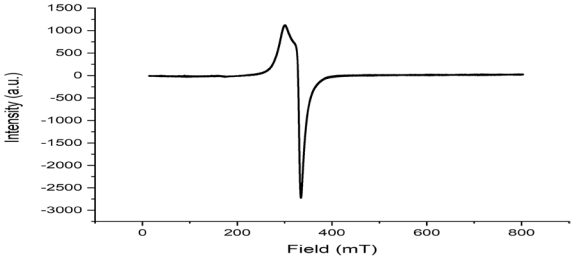

Fig. 4 ESR spectrum of the copper chloride complex

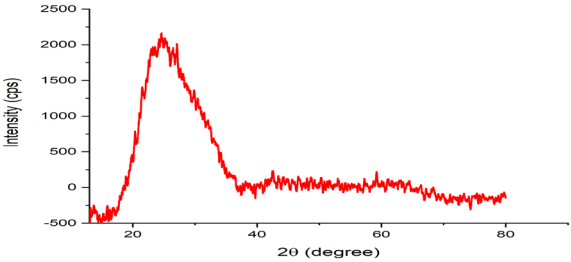

Fig. 5 PXRD spectrum of the copper chloride complex

appearing in the spectra of metal complexes which announces the non-crystalline nature of the compounds (Fig. 5). The amorphous characteristic has been revealed in the studies; hence grain/crystalline was not calculated.

SEM

The Schiff base ligand (NAMB) and the copper chloride (3) complex surface morphology has been deliberated at 15 K magnification scale in which ligand surface morphology displays small rock-like surfaces with pointed edges and distributed randomly with different size matrix. In case of copper chloride complex, a rough surface with a net like matrix was observed as depicted in Fig. 6.

DFT investigations

Geometry optimization

The geometry of the ligand (NAMB) and metal complexes were calculated utilizing density functional theory (DFT) calculations at the B3LYP function and LanL2DZ-theory level Gaussian 09. Figure 7 displays the fully optimized geometry of the ligand and metal complexes. Ligand optimization was performed to investigate geometric and electronic aspects that may influence donation of electron. According to

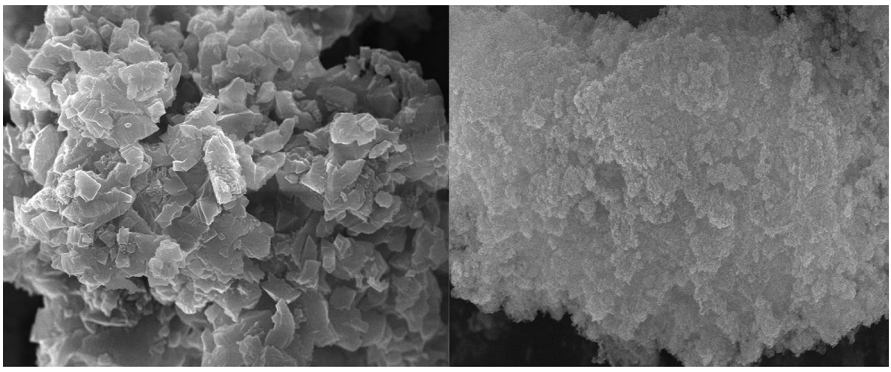

Fig. 6 Surface morphology of the ligand and copper chloride complex

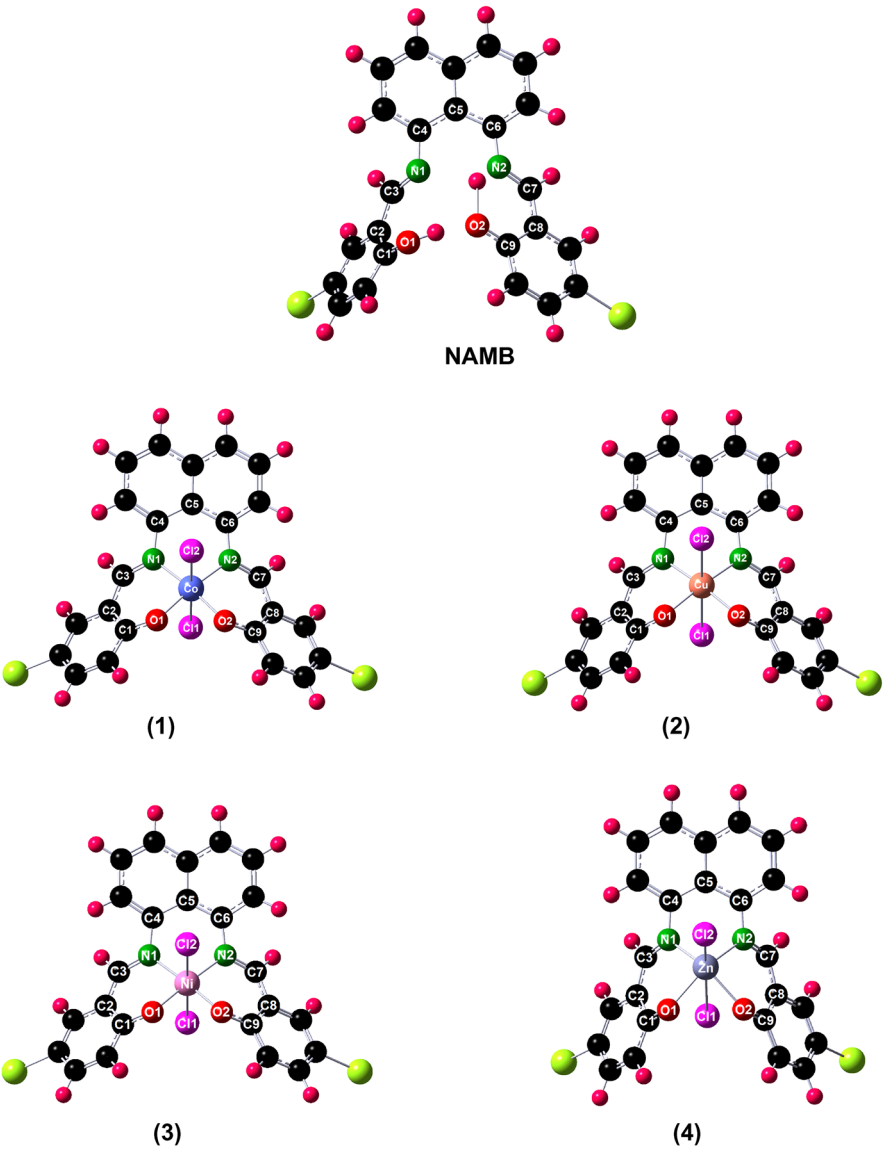

Fig. 7 Optimized geometry of ligand and metal complexes

the computed bond lengths and bond angles, the molecular structure of complexes has octahedral geometry around the Co(II), Cu(II), Ni(II), and Zn(II) centers. The bond lengths and angles of the compounds are enumerated in Table 2. The primary ligand acts as a tetradentate ligand and coordinates with the metal through two imine nitrogen and two hydroxyl oxygen atom. The quantum chemical descriptors were examined implementing optimized geometry of the ligand and complexes.

Table 2 Optimized parameters of ligand (NAMB) and complexes

Parameters	L5 (NAMB)	L5CoCl (1)		L5CuCl (3)		L5NiCl (2)		L5ZnCl (4)	
	Bond length (Å)	Bond length (Å)	Bond angle (°)	Bond length (Å)	Bond angle (°)	Bond length (Å)	Bond angle (°)	Bond length (Å)	Bond angle (°)
C1–C2	1.44	1.45	–	1.46	–	1.44	–	1.48	–
C2–C3	1.47	1.43	–	1.44	–	1.43	–	1.45	–
C3–N1	1.31	1.33	–	1.32	–	1.33	–	1.32	–
C4–N1	1.43	1.43	–	1.42	–	1.43	–	1.43	–
C4–C5	1.45	1.44	–	1.45	–	1.44	–	1.44	–
C5–C6	1.45	1.44	–	1.45	–	1.44	–	1.44	–
C6–N2	1.43	1.43	–	1.42	–	1.43	–	1.43	–
C7–N2	1.34	1.33	–	1.32	–	1.33	–	1.32	–
C7–C8	1.42	1.43	–	1.44		1.43		1.45	
C8–C9	1.46	1.45	–	1.46		1.44		1.48	
C1–O1	1.36	1.34	–	1.31	–	1.33	–	1.30	–
C9–O2	1.31	1.31	–	1.31		1.33		1.29	
M–Cl1	–	2.39	–	2.67	–	2.35	–	2.64	–
M–Cl2	–	2.31	–	2.48	–	2.32	–	2.39	–
O1–M–N1	–	–	92.74	–	91.06	–	91.16	–	84.14
O1–M–N2	–	–	174.10	–	174.08	–	176.51	–	135.56
O1–M–O2	–	–	81.69	–	87.35	–	85.34	–	82.72
O1–M–Cl1	–	–	88.92	–	87.23	–	90.95	–	65.50
O1–M–Cl2	–	–	91.24	–	93.36	–	89.11	–	115.65
N1–M–O2	–	–	174.15	–	174.08	–	176.49	–	84.14
N1–M–N2	–	–	92.76	–	89.94	–	92.33	–	75.27
N1–M–Cl1	–	–	89.19	–	87.0	–	89.96	–	70.44
N1–M–Cl2	–	–	90.64	–	92.43	–	90.99	–	108.33

Table 2 (continued)

Parameters	L5 (NAMB)	L5CoCl (1)		L5CuCl (3)		L5NiCl (2)		L5ZnCl (4)	
	Bond length (Å)	Bond length (Å)	Bond angle (°)	Bond length (Å)	Bond angle (°)	Bond length (Å)	Bond angle (°)	Bond length (Å)	Bond angle (°)
O2–M–N2	–	–	92.74	–	91.06	–	91.17	–	84.13
O2–M–Cl1	–	–	89.19	–	87.23	–	90.94	–	65.46
O2–M–Cl2	–	–	90.64	–	93.36	–	89.11	–	115.65
N2–M–Cl1			88.87		87.0		88.95		70.44
N2–M–Cl2			91.28		92.43		90.99		108.33

Quantum chemical descriptors analysis

The B3LYP function and LanL2DZ basis sets have been employed to investigate the electric and optical parameters of the structure in the frontier molecular orbital (FMO). FMOs are critical components of a molecular structure specifically identified as the lowest unoccupied molecular orbital (LUMO) and the highest occupied molecular orbital (HOMO) as displayed in Fig. 8 [90]. The HOMO inhabited by electrons possesses the potential to donate electrons, while the empty innermost orbital LUMO behave as an electron acceptor. The tendency of a molecule's to provide electrons is directly related to its E_{HOMO}; in general, the higher the HOMO energy (smaller the negative value), the higher the electron-donating capacity [91]. The values of ligand and complexes are shown in Table 3 and determined as follows: the energy difference (ΔE) between the HOMO and LUMO, global softness (S), chemical potential (μ), electronegativity (χ), global hardness (η) and global electrophilicity (ω) [92, 93].

The HOMO and LUMO energies have been employed to assess all reactivity properties. The reactivity and stability of compounds are increased by the increased energy of the smaller band gap. Chemical potential (μ) determines the potential of electrons to deviate from an equilibrium state. A molecule with a negative chemical potential is considered stable and does not spontaneously break down into its individual components. The potential reactivity of the compound is suggested by its low hardness and high softness values. Global electrophilicity (ω) is a functional variable for quantifying the electrophilic reactivity of compounds. An electrophilic molecule has a significant degree of electrophilicity. The presence of a positively charged coordinating metal leads to a reduction in the electronegativity force (χ) of the structures. Electrophilicity is the capability of an electrophile to accumulate extra electronic charge and resist the interchange of electronic charge with the environment. This property is important for understanding both electron transfer (chemical potential) and stability (hardness). Electrophilicity is an important quantum chemical descriptor that serves a major key point in assessing the toxicity of compounds based on their reactivity and site selectivity. The structures exhibit reduced electronegativity (χ) owe to the presence of a positively charged coordinating metal [94].

Molecular electrostatic potential (MEP) of compounds

A crucial quantity that is connected to electron density and is helpful in understanding coordination positions and H-bonding interactions is the MEP. The B3LYP approach, utilizing the LanL2DZ basis set, was employed to compute the MEP-mapped surface of the ligand and complexes. Figure 9 illustrates the MEP maps for the ligand (NAMB) and its complexes. It is evident from the ligand's MEP map that the positive zones were localized over the electropositive area, whereas the negative portions were localized over the electronegative site [95–99].

The O atoms of the phenolic group (deep red/yellow) and the N atoms of the imine moiety are primarily surrounded by the negative regions. The complexes that

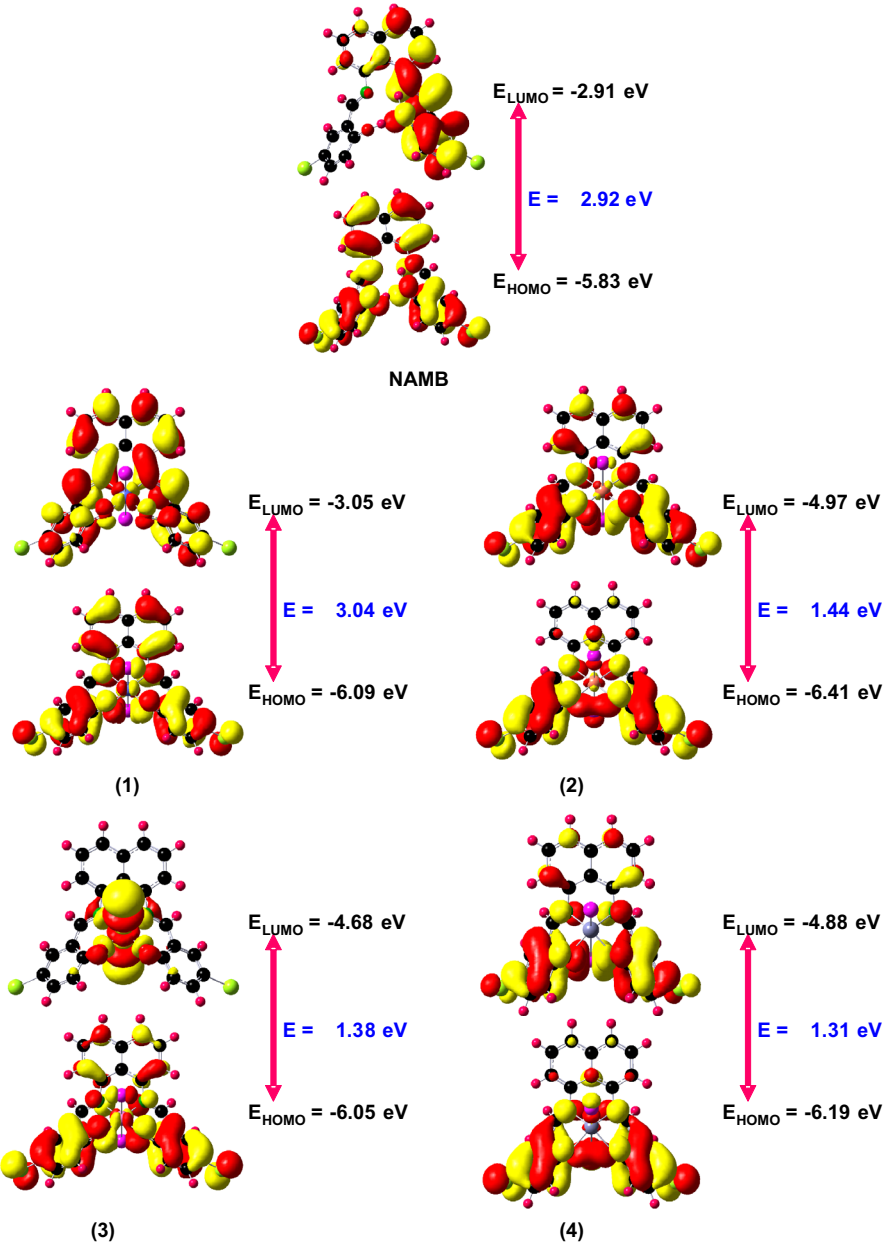

Fig. 8 Frontier molecular orbitals along with band gap (ΔE) of ligand and complexes

exhibit negative region are detected across the chloride atom, the imine moiety N atoms and the O atoms of the phenol group. The most positive areas (blue/green) are observed surrounding the C-atoms of imine moiety and the H atoms of O–H of phenolic group. The bulk of the positive charge is centred over the H and C-atoms. The

Table 3 Estimated DFT parameters with other descriptors

Parameters	NAMB	(1)	(2)	(3)	(4)
Formula weight	524.21	652.03	651.79	656.64	658.48
E (a.u.)	− 1210.28	− 1384.15	− 1408.33	− 1435.13	− 1304.64
HOMO (eV)	− 5.83	− 6.09	− 6.19	− 6.41	− 6.19
LUMO (eV)	− 2.91	− 3.05	− 4.68	− 4.97	− 4.88
ΔE (eV)	2.92	3.04	1.31	1.44	1.31
Global hardness (η)	1.46	1.52	0.69	0.72	0.65
Absolute softness (S)	0.34	0.33	0.72	0.69	0.76
Mulliken electronegativity (χ)	− 4.37	− 4.57	− 5.36	− 5.69	− 5.53
Global electrophilicity (ω)	6.53	6.86	20.87	22.44	23.39
Chemical potential (μ)	4.37	4.57	5.36	5.69	5.53
Dipole moment (Debye)	5.91	5.82	7.22	6.49	7.47

ligand is coordinated with two phenolic O–H and two imine N in complexes because it has four potential coordination sites. Six donor atoms surround the metal ion in an octahedral arrangement. The electrostatic potential at the surface is depicted by various hues. The potential rises in the sequence listed below: Blue > Green > Yellow > Orange > Red [100].

In vitro Biological Studies

Antibacterial studies

The antibacterial in vitro examination was accomplished with gram + ve bacteria (*B. subtilis*, *B. cereus*) as well as gram –ve bacteria (*P. aeruginosa*, *E. coli*), and their minimum inhibitory concentration was assessed [101–103]. The copper chloride (3) complex exhibited maximum effectualness as the least minimum inhibitory concentration was observed against *B. cereus* with 0.0094 µmol/mL. The cobalt chloride (1) complex possess highest efficacy against the *B. subtilis* bacteria with 0.0099 µmol/mL concentration, while copper complex exhibited least MIC value against *E. coli* and *P. aeruginosa* bacterial strains with 0.0189 µmol/mL concentration. Overall, the copper chloride complex (3) was the most proficient antibacterial agent as unveiled in the biological examinations (Table 4, Fig. 10).

Antifungal studies

The antifungal investigation was explored for the synthesized ligand and the metal complex against the selected fungal strains (*C. albicans*, *A. niger*), and minimum inhibitory concentration was examined. The outcome divulges the maximum potency of the copper chloride (3) metal complex against *C. albicans* fungus exhibiting 0.0094 µmol/mL MIC value. While in case of *A. niger*, the cobalt chloride complex (1) displays great efficiency having 0.0198 µmol/mL concentration. The antifungal MIC values were represented in Table 4 and Fig. 11.

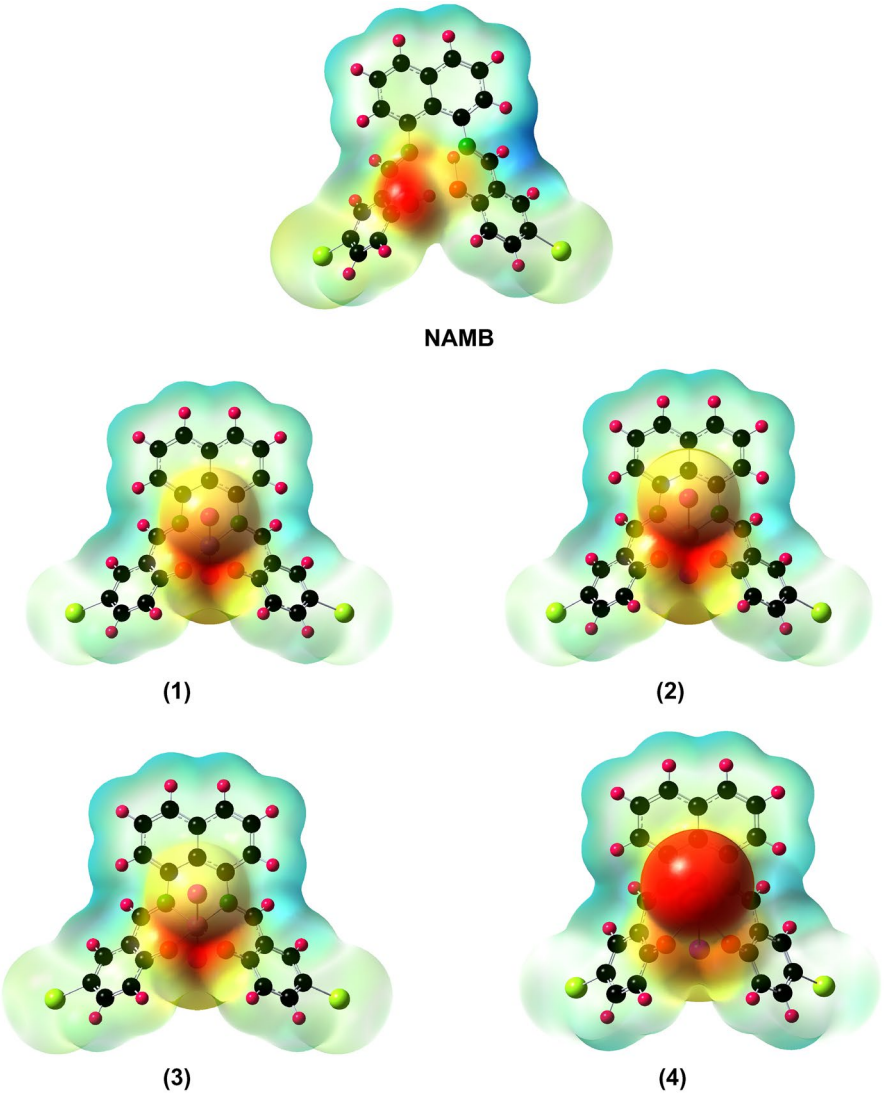

Fig. 9 Molecular electrostatic potential (MEP) analysis ligand and complexes

In silico studies

Molecular docking investigation

The molecular docking was executed for all the synthesized compounds so as to discover pharmacological profile of the compounds. The receptors' protein selected for docking was crystal structure of cholesteryl ester transfer protein (2OBD) that is cholesterol lowering agent [104] and refined 13pf HeLa cell tubulin microtubule

Table 4 MIC values of the synthesized complexes against different microbes

S. no.	MIC (μmol/mL)					
	B. subtilis	*B. cereus*	*E. coli*	*P. aeruginosa*	*A. niger*	*C. albicans*
NAMB	0.049	0.024	0.024	0.049	0.049	0.024
(1)	**0.0099**	0.0198	0.0198	0.0397	**0.0198**	0.0198
(2)	0.0380	0.0191	0.0191	0.0380	0.0380	0.0191
(3)	0.0379	**0.0094**	0.0189	0.0189	0.0379	**0.0094**
(4)	0.0378	0.0189	0.0189	0.0378	0.0378	0.0189
Ciprofloxacin	0.0047	0.0047	0.0047	0.0047	–	–
Fluconazole	–	–	–	–	0.0051	0.0051

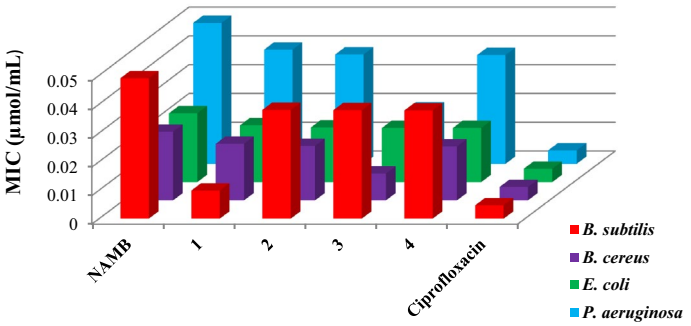

Fig. 10 In vitro antimicrobial results of the compounds

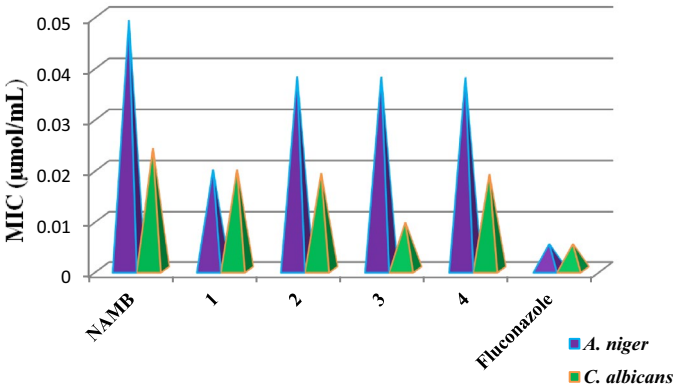

Fig. 11 Antifungal results displaying MIC values of the ligand and metal complexes

(6I2I), which is a receptor of HeLa cells responsible for the cervical cancer in women's [105–109]. The result demonstrates the high effectivity of metal complexes over the ligand as noticed in the data attained from in silico studies. The finding

exemplified that the synthesized compound is more effective against HeLa cancerous cells in comparison to cholesterol receptor because least binding affinity was obtained in case of cancerous cells.

The ligand displays highest binding affinity against both receptors with a binding affinity value of −7.4 kcal/mol and −7.9 kcal/mol for the 2OBD and 6I2I receptors, respectively, while the amino acids which interacts with 2OBD receptor protein was ILE449 via Pi-sigma bonding and with 6I2I receptor via VAL260 (Pi-alkyl), HIS266 (Pi-Pi T-shaped) and ASP199 (Pi-anion) amino acids residues.

The cobalt chloride metal complex exhibits −8.9 kcal/mol binding energy against 2OBD receptor, while interaction displayed were Pi-cation (LYS180), Pi-Pi stacked (TYR144) and Pi-alkyl (LYS180, LEU177, LYS176). The interactions observed with 6I2I receptor were only Pi-alkyl interactions via ALA330, ALA333 and LYS176 amino acid residues possessing the binding energy of −9.6 kcal/mol.

In case of nickel chloride complex, binding affinity obtained was −8.0 kcal/mol and −9.7 kcal/mol with 2OBD and 6I2I receptors correspondingly. The interacting residues with 2OBD receptor were PRO141 (alkyl interaction), LYS185 (pi-alkyl) and also one conventional hydrogen bond with ASN188 amino acid residues, while interaction with 6I2I receptor were alkyl (LYS176, ALA333, ALA330, LYS326) and Pi-anion (ASP211) interactions.

The binding affinity discovered in copper chloride complex against 2OBD and 6I2I receptors were −8.2 kcal/mol and −9.2 kcal/mol, respectively. The interaction noticed were one conventional hydrogen bond via HIS25, Pi-alkyl interaction via HIS25 and alkyl interaction through ALA28 residues against 2OBD receptor. In case of 6I2I receptor, interacting residues were ALA333, LYS176 (alkyl), LYS176 (Pi-alkyl) and one carbon-hydrogen bond through ASP211 amino acid.

The zinc chloride complex possesses −7.8 kcal/mol binding affinity with alkyl interaction (ALA28), Pi-alkyl interactions (ALA28) and Pi-donor hydrogen bond (HIS25) interactions, while in 6I2I receptor, −9.4 kcal/mol binding affinity with Pi-alkyl interaction (PHE214, ALA330, ALA333) and Pi-sigma (PHE214) interactions.

Table 5 displays the binding affinity of the compounds with interacting amino acids, while most proficient compounds interaction was illustrated in Fig. 12. The interaction of other complexes was displayed in Fig. 13

ADME studies

The absorption, distribution, metabolism, excretion and toxicology profile was explored to know the pharmacokinetic characteristics of the compounds (Table 6, Fig. 14). Lipinski rule clearly describes the drug-like characteristics of the

Table 5 Binding affinity and interacting amino acid residues of the compounds

Comp	2OBD		6I2I	
	Binding affinity (Kcal/mol)	Amino acid residue (interacting)	Binding affinity (Kcal/mol)	Amino acid residue (interacting)
NAMB	− 7.4	ILE449	− 7.9	VAL260, HIS266, ASP199
(1)	**− 8.9**	ALA330, ALA333, LYS176	− 9.6	ALA330, ALA333, LYS176
(2)	− 8.0	LYS185, ASN188, PRO141	**− 9.7**	LYS176, ALA333, LYS326, ALA330
(3)	− 8.2	HIS25, ALA28	− 9.2	ALA333, LYS176, ASP211
(4)	− 7.8	ALA28, HIS25	− 9.4	PHE214, ALA330, ALA333, TYR210

complexes. The value of the hydrogen bond acceptors lies below 10 while value of hydrogen bond donor lower than 5 distinctly states the drug characteristics of the compounds and the obtained value of the synthesized compounds varies between 0 and 4 as observed. The value of molar refractivity found in 130.79–146.35 range, and the total polar surface area which demonstrates hydrogen bonding was observed in 43.18–65.18A^{o2}, thereby reflecting the drug profile. The value of bioactivity score was greater than zero for all the compounds which suggests therapeutic potency [110–115].

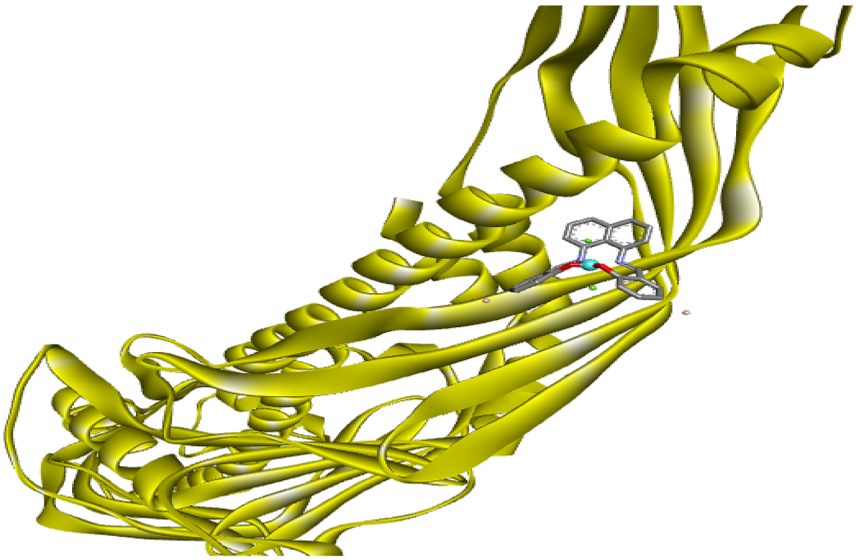

a) Binding site of the cobalt chloride (1) complex with 2OBD receptor

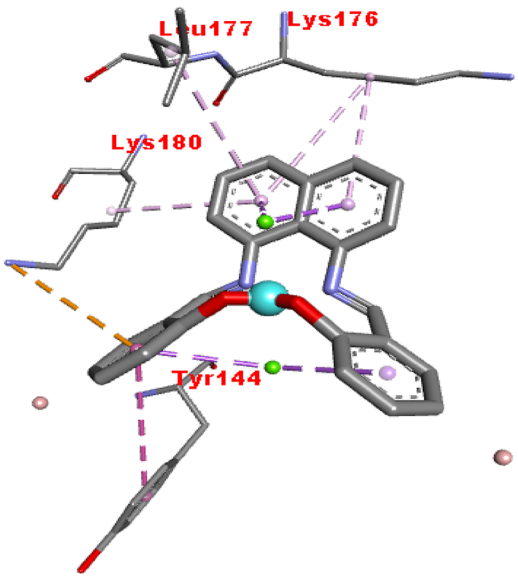

b) 3D Interaction of cobalt chloride (1) complex with 2OBD protein

Fig. 12 Molecular docking interaction of the most potent metal complexes

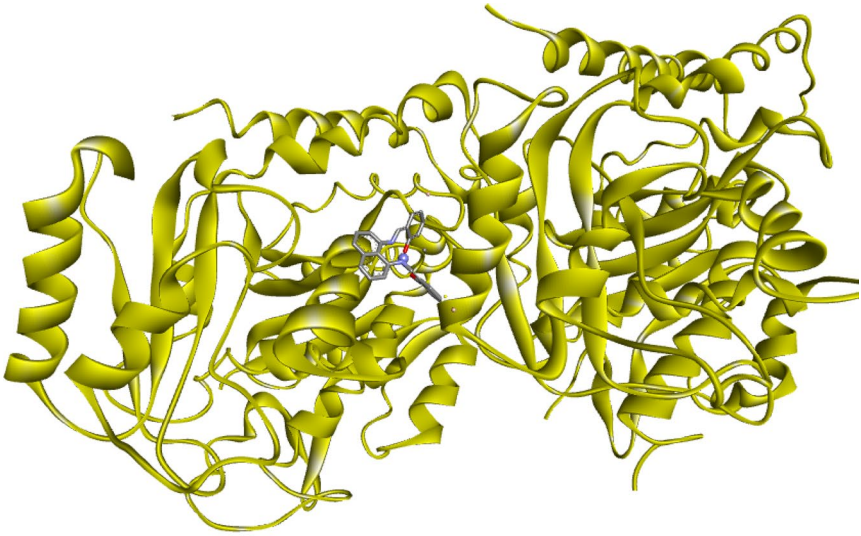

c) Binding site of the nickel chloride (2) complex with 2OBD receptor

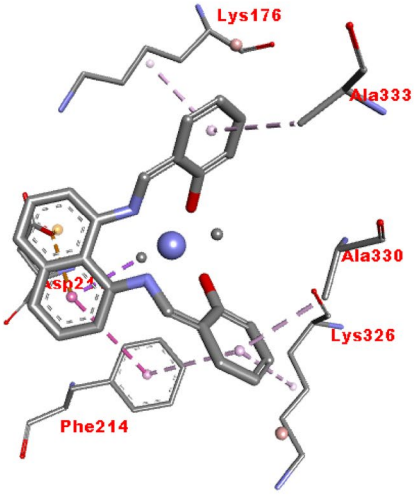

d) 3D Interaction of nickel chloride (2) complex with 6I2I receptor

Fig. 12 (continued)

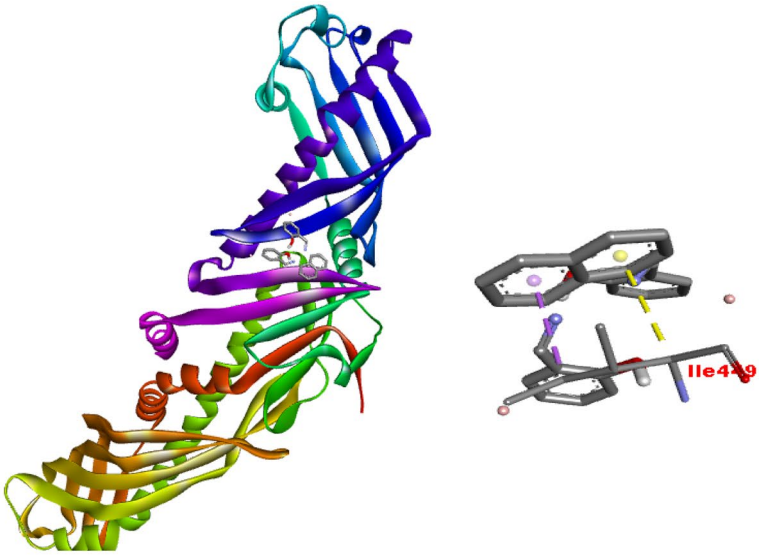

a) Ligand interaction with 2OBD receptor

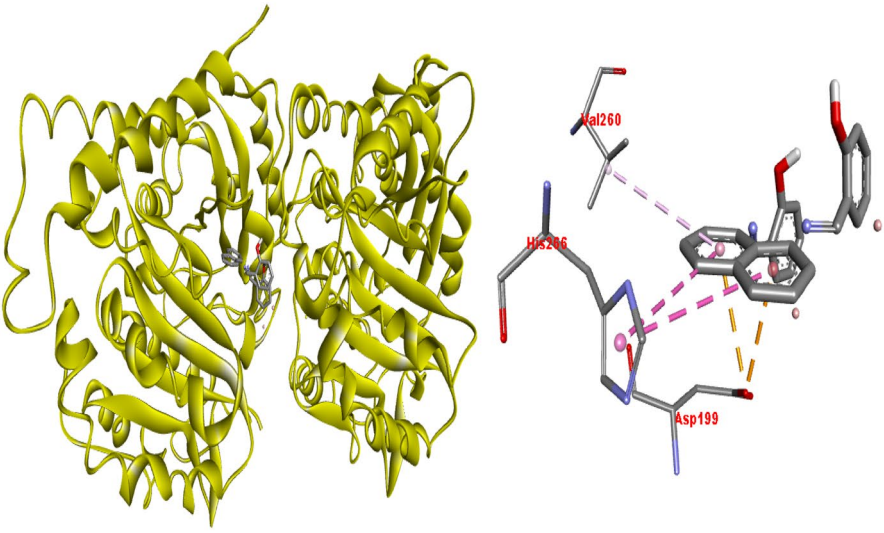

b) Ligand interaction with 6I2I receptor

Fig. 13 Molecular docking interaction of ligand and metal complexes

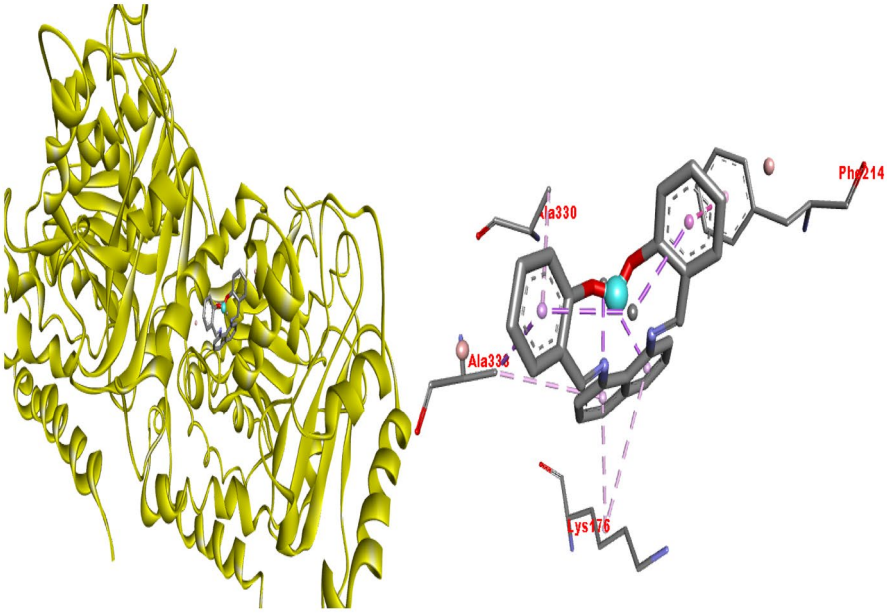

c) Cobalt chloride complex interaction with 6I2I receptor

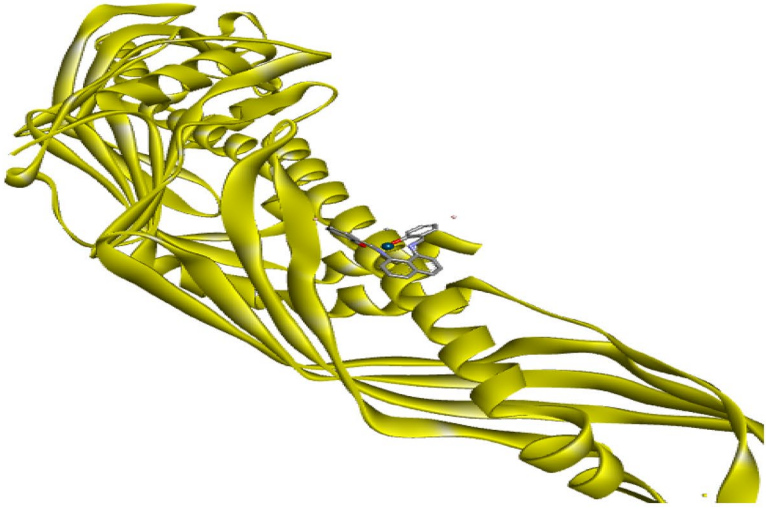

Fig. 13 (continued)

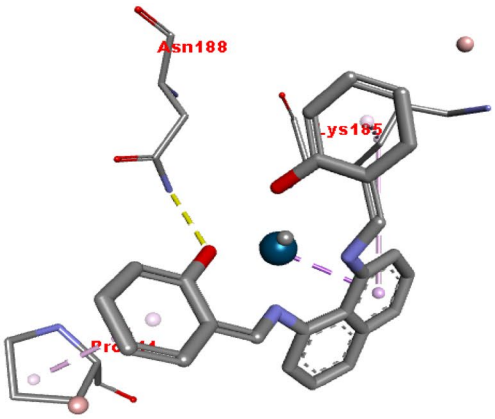

d) Nickel chloride complex interaction with 2OBD receptor

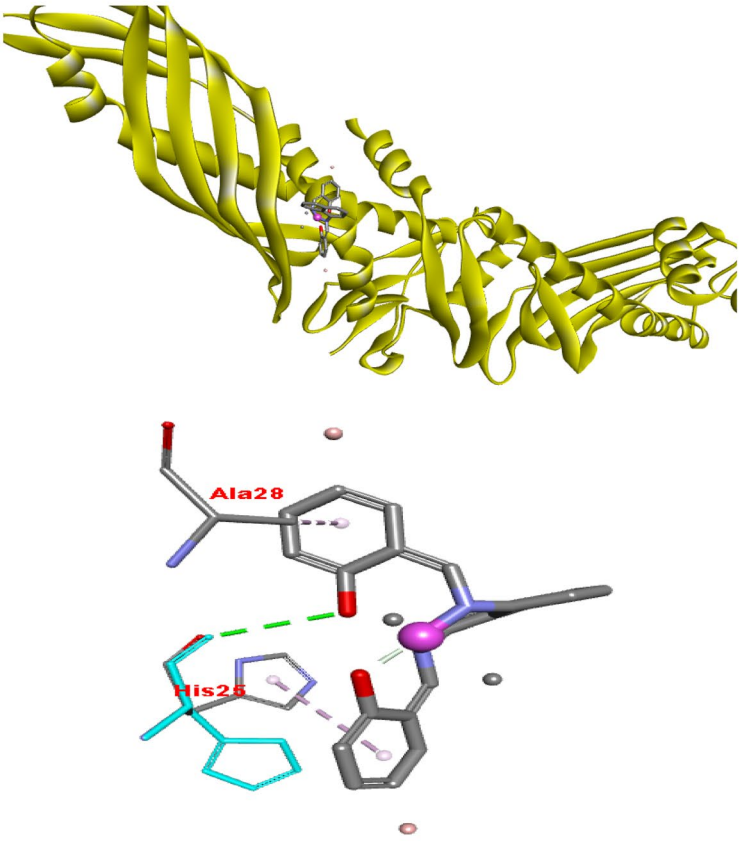

e) Copper chloride complex interaction with 2OBD receptor

Fig. 13 (continued)

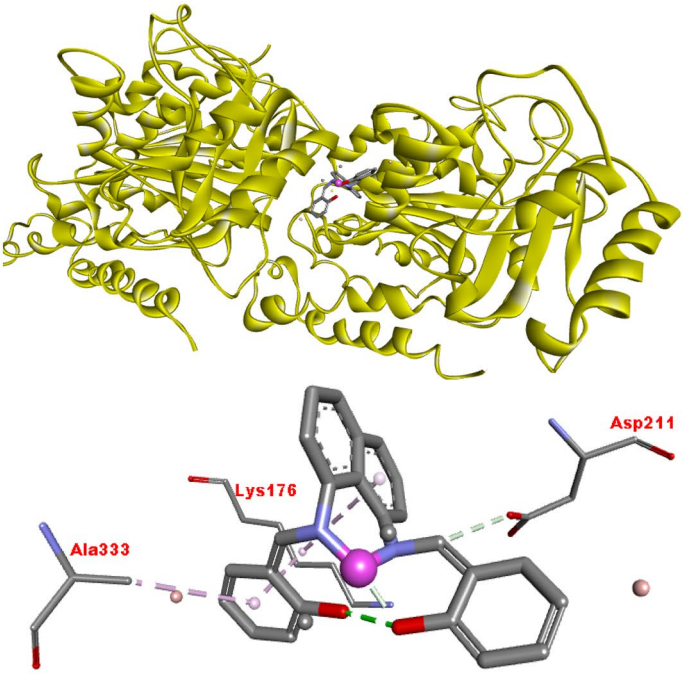

f) Copper chloride complex interaction with 6I2I receptor

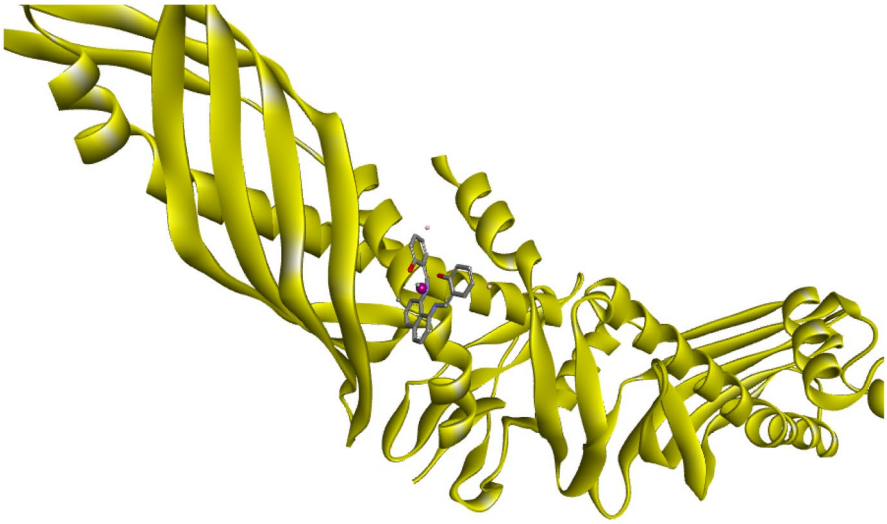

Fig. 13 (continued)

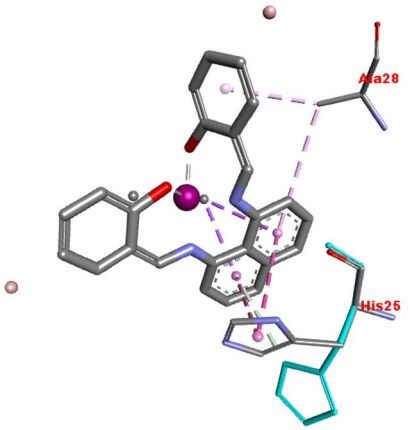

g) Zinc chloride complex interaction with 2OBD receptor

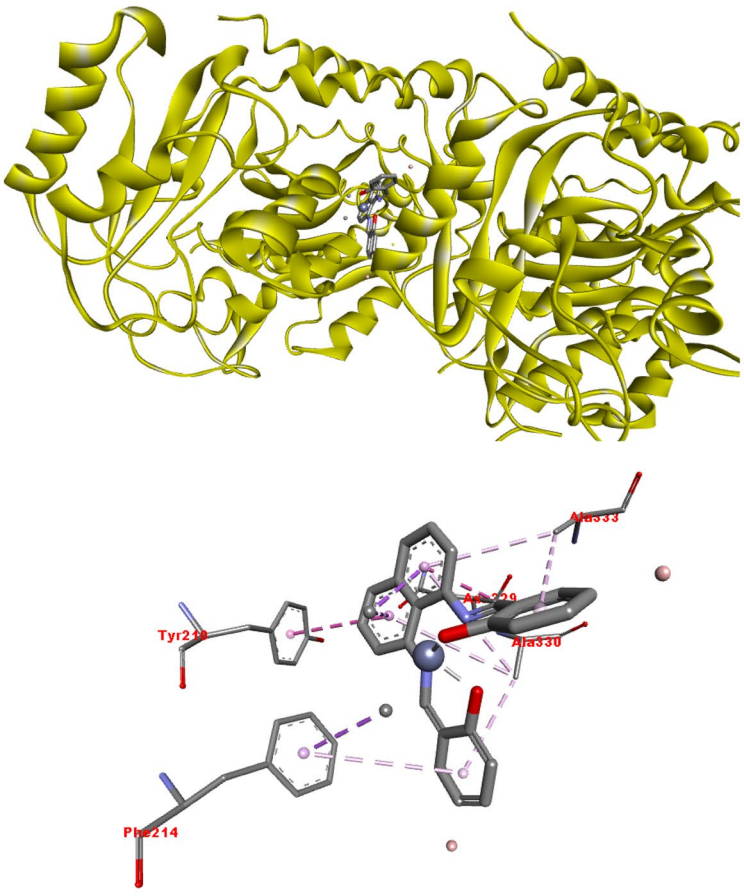

h) Zinc chloride complex interaction with 6I2I receptor

Fig. 13 (continued)

Table 6 Physiochemical parameters of the compounds

Properties	NAMB	(1)	(2)	(3)	(4)
Heavy atoms	22	22	22	22	22
H-bond acceptors	4	2	2	2	2
Molar refractivity	130.79	146.35	146.35	146.35	146.35
No. of H-bond donors	2	0	0	0	0
TPSA	65.18	43.18	43.18	43.18	43.18
No. of rotatable bonds	4	0	0	0	0
Bioactivity score	0.17	0.17	0.17	0.17	0.17
iLogP	3.02	0	0	0	0
GI abs	Low	Low	Low	Low	Low
BBB permeant	No	No	No	No	No
P-gp subs	Yes	Yes	Yes	Yes	Yes
Log Kp	−4.93	−4.41	−4.41	−4.41	−4.41
Pains	0	0	0	0	0
Synth. access	3.05	4.21	3.91	4.24	4.30

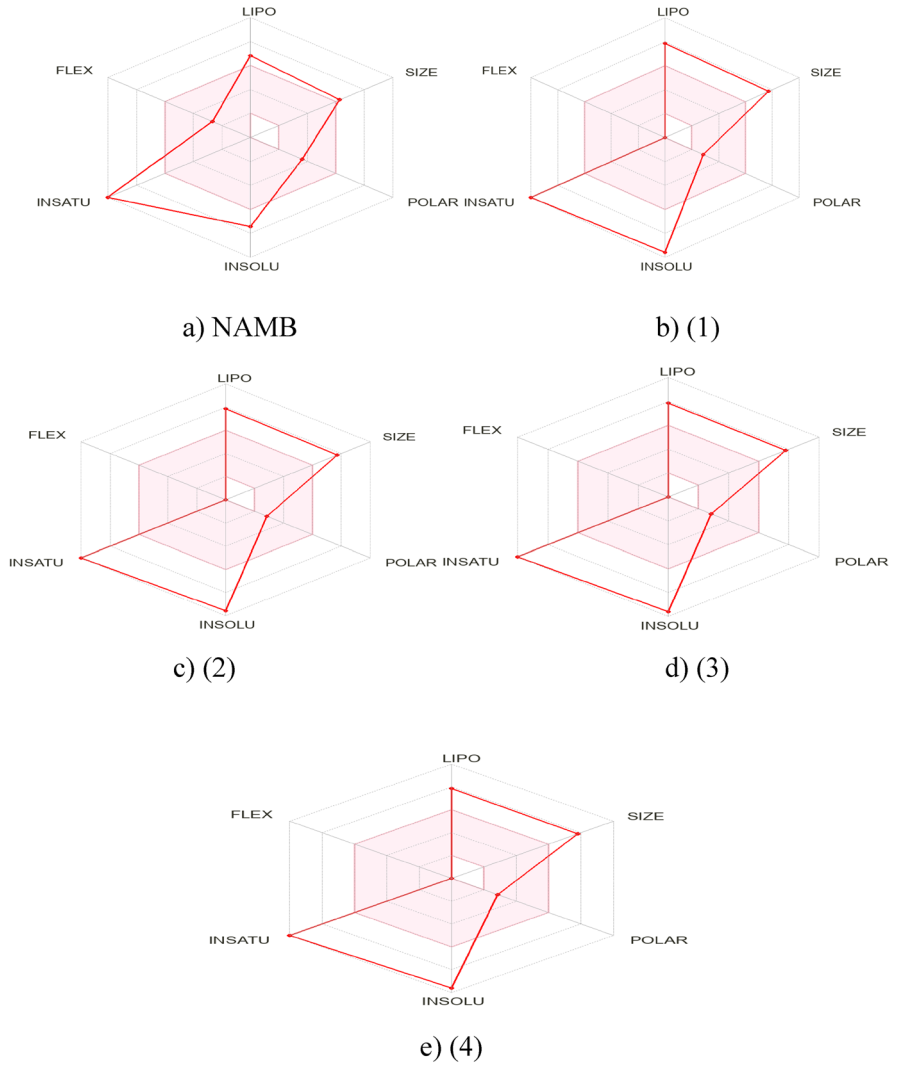

Fig. 14 Radar diagram of the ligand and metal complexes

Conclusions

The novel Schiff base ligand and their transition metal complexes were fabricated via well-known condensation method, and the structure elucidation has been performed employing various techniques. The spectral examination and computational studies unveils the octahedral geometry encircling the metal complexes. In vitro antimicrobial investigation has been assessed to gauze the biological effectualness of the fabricated compounds and the outcomes exposes the copper chloride complexes as most proficient antimicrobial agent, while the least efficacy was divulged in case of the ligand. The nickel chloride complex has been pronounced to be more effective on HeLa cancerous cells as revealed in the docking analysis. Furthermore, docking on cholesteryl ester receptor protein recommends the potential implementations of the synthesized complexes as cholesterol lowering agent.

Acknowledgements The authors highly acknowledge SAIF-IIT Bombay, MNIT Jaipur, for providing analytical facility and SAIF-IIT Bombay for ESR facility.

Author contributions I.S. done data curation, writing—original draft preparation, investigation, visualization; A.S. contributed to conceptualization, methodology, project administration, validation, writing—review & editing, supervision; Y.D. and J.S.K. done data curation and writing—original draft preparation.

Funding The research work has received financial support from the Council of Scientific and Industrial Research-University Grants Commission (CSIR-UGC), New Delhi, in form of JRF fellowship with Reference Number 231610039634.

Data availability Data supporting the results of this study are available on fair request from the corresponding author.

Declarations

Conflict of interest The authors declare no conflict of interests.

References

1. M. Rajasekar, S. Sreedaran, R. Prabu, V. Narayanan, R. Jegadeesh, N. Raman, A.K. Rahiman, J. Coord. Chem. **63**, 136 (2010)
2. C.J. Dhanaraj, M.S. Nair, J. Coord. Chem. **62**, 4018 (2009)
3. M.S. Karthikeyan, D.J. Prasad, B. Poojary, K.S. Bhat, B.S. Holla, N.S. Kumari, Bioorg. Med. Chem. **14**, 7482 (2006)
4. P. Panneerselvam, R.R. Nair, G. Vijayalakshmi, E.H. Subramanian, S.K. Sridhar, Eur. J. Med. Chem. **40**, 225 (2005)
5. N.C. Gianneschi, S.T. Nguyen, C.A. Mirkin, J. Am. Chem. Soc. **127**, 1644 (2005)
6. A. Houlton, N. Jasim, R.M. Roberts, J. Silver, D. Cunningham, P. McArdle, T. Higgins, J. Chem. Soc. Dalton Trans. **14**, 2235 (1992)
7. K.S. Murray, Adv. Inorg. Chem. **43**, 261 (1995)
8. J.W. Lu, Y.H. Huang, S.I. Lo, H.H. Wei, Inorg. Chem. Commun. **10**, 1210 (2007)
9. J. Gradinaru, A. Forni, V. Druta, F. Tessore, S. Zecchin, S. Quici, N. Garbalau, Inorg. Chem. **46**, 884 (2007)
10. E. Basaran, H.G. Sogukomerogullari, R. Cakmak, S. Akkoc, T.T. Tok, A. Kose, Bioinorg. Chem. **129**, 106176 (2022)
11. A. El-Sonbati, M. El-Mogazy, S. Nozha, M. Diab, M. Abou-Dobara, A. Eldesoky, S.M. Morgan, J. Mol. Struct. **1248**, 131498 (2022)

12. H.Y. Khan, S. Parveen, I. Yousuf, S. Tabassum, F. Arjmand, Coord. Chem. Rev. **453**, 214316 (2022)
13. O.A. Dar, S.A. Lone, M.A. Malik, F.M. Aqlan, M.Y. Wani, A.A. Hashmi, A. Ahmad, Heliyon **5**, e02055 (2019)
14. H.M.A. El-Lateef, A.M. Ali, M.M. Khalaf, A. Abdou, Bull. Chem. Soc. Ethiop. **38**(1), 147 (2024)
15. A.M. Abu-Dief, M.A. Said, O. Elhady, N. Alahmadi, S. Alzahrani, T.N.A. Eskander, M.A.E.A.A. Ali, Inorg. Chem. Commun. **155**, 110955 (2023)
16. H.M.A. El-Lateef, A.M. Ali, M.M. Khalaf, A. Abdou, Bull. Chem. Soc. Ethiop. **38**(2), 397 (2024)
17. A. Singh, R.C. Ahirwar, K.K. Borgaonkar, N. Gupta, M. Ahsan, J. Rathore, P. Das, S. Ganguly, R. Rawat, Molecules **28**(10), 4182 (2023)
18. M.A.E.A.A.A. El-Remaily, O. Elhady, T.N.A. Eskander, S.K. Mohamed, A.M. Abu-Dief, Sohag J. Sci. **9**, 7 (2024)
19. H.A. Hasan, S.M. Mahdi, H.A. Ali, Bull. Chem. Soc. Ethiop. **38**, 99 (2024)
20. A. Singh, A. Chaudhary, J. Iran. Chem. Soc. **17**(4), 1 (2019)
21. S. Pramanik, A. Singh, B.A. Abualsoud, A. Deepak, P. Nainwal, A.S. Sarsgsyan, S. Bellucci, RSC Adv. **14**(5), 3209 (2024)
22. A. Singh, S. Gnanvel, Supriya, AI, S.P. Diwan, A. Unnisa, C.K. Dixit, K. Pant, ICBECT 2603 (2023)
23. D. Bissett, K. McLaughlin, L. Kelland, R. Brown, Br. J. Cancer **67**, 742 (1993)
24. M.E. Bianchi, M. Beltrame, G. Paonessa, Science **243**, 1056 (1989)
25. T.A. Yousef, A.S. Al-Janabi, Heliyon **10**, e37310 (2024)
26. M. Turkmenoglu, S.T. Yildirim, A. Ataly, B. Turkmenoglu, Chem. Sel. **9**, e202303519 (2024)
27. U. Dasmahapatra, B. Maiti, M.M. Alam, K. Chanda, Europ. J. Med. Chem. **275**, 116603 (2024)
28. A.O. Keikha, S. Shahraki, E. Dehghanian, H.M. Torshizi, Spectrochim Acta Part A: Mol. Biomol. Spectrosc. **325**, 125034 (2024)
29. S. Masood, U.M. Babar, M. Ashfaq, M. Tahir, M.N.N. Zafar, New J. Chem. **47**, 21845 (2023)
30. W.A. Siddiqui, M.A. Raza, A. Ashraf, M. Ashfaq, M.N. Tahir, S. Niaz, J. Mol. Struct. **1295**, 136603 (2024)
31. S. Masood, M. Jamshaid, M.N. Zafar, E.U. Mughal, M. Ashfaq, M.N. Tahir, J. Mol. Struct. **1295**, 136571 (2024)
32. H. Kargar, M. Fallah-Mehrjardi, M. Ashfaq, K.S. Munawar, M.N. Tahir, J. Mol. Struct. **1294**, 136458 (2023)
33. E. Alaman, A. Agar, M. Tahir, M. Ashfaq, E. Poyraz, N. Dege, J. Struct. Chem. **64**, 1314 (2023)
34. Q. Aliyeva, M. Tahir, M. Ashfaq, K. Munawar, S. Rahmanova, U. Hasanova, A. Rustamova, H. Mammadova, E. Movsumov, J. Struct. Chem. **64**, 995 (2023)
35. I. Sindhu, A. Singh, Nanotechnology: A boon for the scientific domain, pp. 1–15 (IIP Series, 2024). https://doi.org/10.58532/V3BECS22P1CH1.
36. P. Bera, P. Brandão, G. Mondal, H. Jana, A. Jana, A. Santra, P. Bera, Polyhedron **134**, 230 (2017)
37. A. Divsalar, A.A. Saboury, L. Ahadi, E. Zemanatiyar, H. Mansouri-Torshizi, BMB Rep. **43**, 766 (2010)
38. R. Farghadani, H.Y. Lim, M.A. Abdulla, J. Rajarajeswaran, Bioorg. Chem. **152**, 107730 (2024)
39. M. Jiang, X. Su, X. Zhong, Y. Lan, F. Yang, Y. Qin, C. Jiang, J. Mol. Struc. **1318**, 139403 (2024)
40. S. Adhikari, P. Nath, A. Das, A. Datta, N. Baildya, A.K. Duttaroy, S. Pathak, Biomed. Pharma **171**, 116211 (2024)
41. M. Rabiee, M. Salehi, M. Kubicki, A. Khaleghian, M. Iraji, J. Mol. Struct. **1302**, 137495 (2024)
42. L. Tabrizi, H. Chiniforoshan, H. Tavakol, Spectrochim Acta Part A **141**, 16 (2015)
43. S. Kumar, D.N. Dhar, P. Saxena, J. Sci. Ind. Res. **68**, 181 (2009)
44. Z. Akbari, M. Montazerozohori, S.J. Hoseini, R. Naghiha, P. Hayati, G. Bruno, A. Santoro, J.M. White, Appl. Organomet. Chem. **35**, e6181 (2021)
45. S. Gurusamy, M. Sankarganesh, R. NandiniAsha, A. Mathavan, J. Biomol. Struct. Dyn. **41**, 599 (2023)
46. M. Chen, J. ShangGuan, J. Jiang, J. Jiang, F. Li, Q. Dong, H. Diao, X. Liu, Int. J. Biol. Macromol. **227**, 1078 (2023)
47. N. Raman, S. Thalamuthu, J. Dhaveethuraja, M. Neelakandan, S. Banerjee, J. Chil. Chem. Soc. **53**, 1439 (2008)
48. I. Kostova, L. Saso, Curr. Med. Chem. **20**, 4609 (2013)

49. A. Fetoh, O.A. El-Gammal, G.M.A. El-Reash, J. Mol. Struct. **1173**, 100 (2018)
50. G. Matela, Med. Chem. (Former. Curr. Med. Chem.-Anti-Cancer Agent.) **20**, 1908 (2020)
51. Z.Y. Yang, R.-D. Yang, F.-S. Li, K.-B. Yu, Polyhedron **19**, 2599 (2000)
52. V. Bressi, Z. Akbari, M. Montazerozohori, A. Ferlazzo, D. Iannazzo, C. Espro, G. Neri, Sensors **22**, 900 (2022)
53. Z. Akbari, M. Montazerozohori, G. Bruno, K. Moulaee, G. Neri, Appl. Organomet. Chem. **36**, e6610 (2022)
54. Z. Akbari, C. Stagno, N. Irai, T. Efferth, E.A. Omer, A. Piperno, M. Montazerozohori, M. Feizi-Dehnayebi, N. Micale, J. Mol. Struct. **1301**, 137400 (2024)
55. M.S. Rana, M.A. Islam, M.S. Islam, M.S. Sarafi, M.K. Zahan, M.F. Hossen, M.A. Asraf, Appl. Organomet. Chem. (2024). https://doi.org/10.1002/aoc7724
56. P. Saran, D. Vishnu, S. Parveen, A. Kosiha, S. Dharani, G. Kalaiarasi, Inorg. Chim. Acta **565**, 121997 (2024)
57. E.S. Aazam, M. Majrashi, M.A. Hussien, Heliyon **10**, e37385 (2024)
58. A.C. Ekennia, A.A. Osowole, L.O. Olasunkanmi, D.C. Onwudiwe, E.E. Ebenso, Res. Chem. Intermed. **43**, 3787 (2017)
59. R.F.M. Elshaarawy, F.H.A. Mustafa, A.R. Sofy, A.A. Hmed, C. Janiak, J. Environ. Chem. Eng. **7**, 102800 (2018)
60. B. Islam, C. Sharma, A. Adem, E. Aburawi, S. Ojha, Dev. Ther. **9**, 4943 (2015)
61. I. Sindhu, A. Singh, Res. Chem. Intermed. **50**, 413 (2023)
62. O.E. Gammal, F.S. Mohamed, G.N. Rezk, A.A. El-Bindary, J. Mol. Liq. **326**, 1115223 (2021)
63. L. Ghasemi, M.H. Esfahani, U. Sahebi, A. Divsalar, A. Abbasi, M. Behzad, J. Mol. Struct. **1294**, 136568 (2023)
64. M. Pichandi, S. Shanmugam, J. Mol. Struct. **1307**, 137932 (2024)
65. S. Thanigachalam, M. Pathak, RSC Adv. **14**, 13062 (2024)
66. H. Howsaui, A.A. Sharfalddin, M.H. Abdellattif, A.S. Basaleh, M.A. Hussien, Appl. Sci. **11**, 9067 (2010)
67. O. Trott, A.J. Olson, J. Comput. Chem. **31**, 455 (2010)
68. T. Manjuraj, T.C.M. Yuvaraj, N.D. Jayanna, M.S. Sarvajith, Mat Today Proceed. Mat Today proceed. **54**, 646 (2021)
69. M. Gulcan, M. Sonmez, I. Berber, Turk. J. Chem. **36**, 189 (2021)
70. M.J. Frisch, G.W. Trucks, H.B. Schlegel, G.E. Scuseria, M.A. Robb, J.R. Cheeseman et al., Gaussian 09 Revision B.01 (Gaussian Inc Wallingford, 2010).
71. B. Miehlich, A. Savin, H. Stoll, H. Preuss, Chem. Phys. Lett. **157**, 200 (1989)
72. C. Singh, D. Adhikari, B.K. Singh, Polyhedron **259**, 117050 (2024)
73. N.H. Boukoucha, Z. Messasma, D. Aggoun, Y. Quennoughi, C. Bensouici, M. Garcia, D. Lopez, M. Guelfi, F. Marchetti, G. Bresciani, Z. Chorfi, J. Mol. Struct. **1319**, 139505 (2024)
74. C. Lee, W. Yang, R.G. Parr, Phys. Rev. B **37**, 785 (1988)
75. H. Ali, A. Anjum, D. Goswami, J. Mol. Struct. **1307**, 138039 (2024)
76. N.H. Mahmoud, G.H. Elsayed, A. Aboelnaga, A.M. Fahim, Appl. Organomet. Chem. **1**, e6697 (2022)
77. P.J. Hay, W.R. Wadt, J. Chem. Phys. **82**, 270 (1985)
78. R.K. Mohapatra, A.K. Sarangi, M. Azam, M.M. El-Ajaily, M.K. E-Zahan, S.B. Patjoshi, D.C. Dash, J. Mol. Struct. **1179**, 65 (2019)
79. D. Ramakrishna, B.R. Bhat, R. Karvembu, Catal. Commun. **11**, 498 (2010)
80. W.H. Mahmoud, M. Bayomi, M. ElMosallamy, A.A. El-Sherif, Egyp. J. Chem. **67**, 379 (2024)
81. A.M. Belal, I.M. El-Deen, N.Y. Farid, R. Zakaria, M.S. Refat, Spectrochim. Acta Part A **149**, 771 (2015)
82. G. Venkatesh, P. Vennila, S. Kaya, S.B. Ahmed, P. Sumathi, V. Siva, P. Rajendran, C. Kamal, ACS Omega **9**, 8123 (2024)
83. Z. Li, S. Wu, H. Ding, D. Zheng, J. Hu, X. Wang, Q. Kan, New J. Chem. **37**, 1561 (2013)
84. N. Turan, H. Seymen, B. Gunduz, K. Buldurun, N. Colak, Optic Mat. **148**, 114802 (2024)
85. A. Allahresani, J. Iran. Chem. Soc. **14**, 1051 (2017)
86. Y. Zhu, Y. Jiao, D. Lu, Y. Cheng, A. Jia, Q. Zhang, J. Coord. Chem. **77**, 295 (2024)
87. M. Aghajani, E. Safaei, B. Karimi, Synth. Met. **233**, 63 (2017)
88. N.P. Ndahi, H. Garba, I. Waziri, A.A. Osunlaja, H.A. Putaya, Niger. J. Pharmaceu Biomed. Res. **3**, 53 (2018)

89. P. Bhunia, S. Dutta, S. Maity, J. Mayans, A. Escuer, A. Ghosh, Inorg. Chim. Acta **545**, 121264 (2023)
90. A.A. Alothman, Z.M. Almarhoon, J. Mol. Struct. **1206**, 127704 (2020)
91. L.P. Nitha, R. Aswathy, N.E. Mathews, B.S. Kumari, K. Mohanan, Spectrochim Acta Part A: Mol. Biomol. Spectrosc. **118**, 154 (2014)
92. C. Alaşalvar, M.S. Soylu, H. Unver, N.O. Iskeleli, M. Yildiz, M. Ciftci, E. Banoglu, Spectrochim Acta A Mol. Biomol. Spectrosc. **132**, 555 (2014)
93. M.H. Abdel-Rhman, A.A. El-Asmy, R. Ibrahim, N.M. Hosny, J. Mol. Struct. **1279**, 135023 (2023)
94. J.S. Kirar, S. Khare, N. Tiwari, Chem. Sel. **6**, 11557 (2021)
95. T.L. Yusuf, S.D. Oladipo, S. Zamisa, H.M. Kumalo, I.A. Lawal, M.M. Lawal, N. Mabuba, ACS Omega **6**, 13704 (2021)
96. S.N. Shukla, P. Gaur, M.L. Raidas, B. Chaurasia, J. Mol. Struct. **1202**, 127362 (2020)
97. Y. Deswal, S. Asija, D. Kumar, D.K. Jindal, G. Chandan, V. Panwar, S. Saroya, N. Kumar, Res. Chem. Intermed. **48**, 703 (2022)
98. Y. Deswal, S. Asija, A. Dubey, L. Deswal, D. Kumar, D.K. Jindal, J. Devi, J. Mol. Struct. **1253**, 132266 (2022)
99. Y. Deswal, S. Asija, A. Tufail, A. Dubey, L. Deswal, N. Kumar, S. Saroya, J.S. Kirar, N.M. Gupta, Appl. Organomet. Chem. **37**, e7050 (2023)
100. Y. Deswal, S. Asija, A. Tufail, A. Dubey, L. Deswal, N. Kumar, J.S. Kirar, N.M. Gupta, P. Barwa, J. Inorg. Organomet. Polym. Mater. **34**, 144 (2024)
101. I. Rajaei, S.N. Mirsattari, Polyhedron **102**, 479 (2015)
102. V. Rangaswamy, S. Renuka, I. Venda, Mater. Today Proc. **51**, 1810 (2022)
103. J. Saranya, S.J. Kirubabathy, S. Chitra, A. Zarrouk, K. Kalpana, K. Lavanya, B. Ravikiran, Arab. J. Sci. Eng. **45**, 4683 (2020)
104. K.R.S. Gowda, H.S.B. Naik, B.V. Kumar, C.N. Sudhamani, H.V. Sudeep, T.R.R. Naik, G. Krishnamurthy, Spectrochim Acta **105**, 229 (2013)
105. T.J. Saritha, P. Metilda, J. Saudi Chem. Soc. **25**, 101245 (2021)
106. L.H. Abdel-Rahman, M.S.S. Adam, N. Al-Zaqri, M.R. Shehata, H.E. Ahmed, S.K. Mohamed, Arab. J. Chem. **15**, 103737 (2022)
107. P. Arthi, M. Dharmasivam, B. Kaya, A.K. Rahiman, Bio. Interact. **373**, 110349 (2023)
108. A.Z. El-Sonbati, M.A. Diab, A.M. Eldesoky, S.M. Morgan, O.L. Salem, Appl. Organomet. Chem. (2019). https://doi.org/10.1002/aoc.4839
109. A.Z. El-Sonbati, M.A. Diab, S.M. Morgan, M.I. Abou-Dobara, A.A. El-Ghettany, J. Mol. Struct. **1200**, 127065 (2019)
110. C.A. Lipinski, F. Lombardo, B.W. Dominy, P.J. Feeney, Adv. Drug Deliv. Rev. **46**, 3 (2001)
111. K.J. Babu, D. Ayodhya, Res. Chem. **6**, 101110 (2023)
112. Y. Belay, A. Muller, F.S. Mokoena, A.S. Adeyinka, R. Motadi, A.K. Oyebamji, Sci. Rep. **14**, 6951 (2024)
113. U. Yasar, I. Gonul, C. Turkes, Y. Demir, S. Beydemir, Chem. Sel. **6**, 7278 (2021)
114. S.M. Morgan, M.A. Diab, A.Z. El-Sonbati, Appl. Organomet. Chem. **32**, e4305 (2018)
115. M.A. Bourouai, A. Bouchoucha, K.S. Larbi, S. Cosnier, S. Djebbar, Polyhedron **253**, 116914 (2024)

Authors and Affiliations

Indu Sindhu[1] · Anshul Singh[1] · Yogesh Deswal[2] · Jagat Singh Kirar[3]

✉ Anshul Singh
anshul9008@gmail.com

Indu Sindhu
indusindhu22@gmail.com

Yogesh Deswal
deshwalyogesh72@gmail.com

Jagat Singh Kirar
j.skirar007@gmail.com

[1] Department of Chemistry, Baba Mastnath University, Rohtak 124021, India

[2] Department of Chemistry, Central University of Haryana, Mahendergarh 123031, India

[3] Department of Chemistry, Govt. P. G. College, Guna, M.P. 473001, India